

Failure modes of loose landslide deposits in the 2008 Wenchuan earthquake area in China

Jianjun Gan^{1,2}, Yi Xia Zhang²

¹National-Local Joint Engineering Laboratory of Water Engineering Safety and Efficient Utilization of Resources in Poyang Lake Watershed. Nanchang Institute of Technology, Nanchang, 330099, Jiangxi, China

²School of Computing, Engineering and Mathematics, Western Sydney University, 2751, NSW, Australia.

Correspondence to: Jianjun Gan (ganjianjun@nit.edu.cn)

Abstract: In this study, a geological investigation and statistical analysis of the postearthquake slope deposit failures in a meizoseismal area were presented with a selected example from the 2008 Ms 8.0 Wenchuan earthquake that occurred in Sichuan Province in China. The typical slope deposit failures were surveyed in three meizoseismal areas, namely, Qingchuan County in Guangyuan city, Beichuan County in Mianyang city, and the epicenter area, Wenchuan County, in Aba Tibetan Autonomous Prefecture. According to the movement, materials and deformation mechanisms of the rock or soil, the failures of the postearthquake landslide deposits could be subdivided into four categories: slide, rockfall, erosion and flow. This classification of the failure modes of landslide deposits considers topography and failure after an earthquake. Other important factors, such as topography, lithology and hydrogeology, are also considered. The above-mentioned four failure categories are further split into 12 subclassifications. The complicated deformation mechanisms and different failure patterns of the slope deposits are analyzed for typical deposits. This classification provides a good reference for the prediction of geological hazards, and the mitigation of the landslides and debris flows caused by loose deposits in meizoseismal areas is still a difficult task.

1. Introduction

The failure types of postearthquake deposits have been examined in several studies, and classification (1938) is primarily based on the materials (earth and rock), movement (flow and slip) and velocity (slow or very rapid) without considering the effects of the topography, landform, volume and inducing mechanism. Based on the material and type of movement, Varnes (1954, 1978) classified the slope failure into five types, including fall, topple, slide, spread and

35 flow, and this has been the most widely used classification for landslides in the world. According
36 to the seismic parameters, materials and geological environment, Keefer (1984) divided
37 landslides into 14 types. Considering the landslide shape and geotechnical parameters,
38 Hutchinson (1988) divided the slope deformation failure modes into a creep, frozen ground
39 phenomena, and landslides but did not consider the trigger mechanisms and the effects of the
40 volume. Hungr (2001) classified landslides into ten types based on genetic and morphological
41 characteristics and introduced a new category in combination with unsorted material and sorted
42 material. However, the deformation failure modes and the particularity of the loose
43 postearthquake main body have not been extensively researched in previous studies, and further
44 studies should be conducted based on these landslide classifications.

45 The purpose of the new classification proposed in this paper is to effectively split landslide
46 deposits into common categories according to deformation mechanisms, which retains the
47 established concept and reveals the deformation and failure trends of landslide events. This
48 approach is easy to implement with a statistical analysis of field surveys, without resorting to
49 more complex taxonomic methods. Moreover, understanding the deformation and failure modes
50 can help to mitigate and prevent similar geological disasters. Some authors have made good
51 attempts and achieved significant results. For instance, the “locking section” was used by Huang
52 (2011) in one study of the mechanisms of large-scale landslides that occurred in China to identify
53 a three-section model that includes sliding, tension cracking and shearing. Using the same
54 apparatus, Yang (2015) also evaluated the postearthquake rainfall-triggered deposit failure that
55 occurred in the Lushan area, Sichuan Province, China.

56 The discussion in this paper focuses on the deformation and failure mechanism of loose deposits
57 after an earthquake. Although the deformation and damage mechanisms of the accumulation body
58 have been preliminarily considered, the classification and specifics of the landslide deposits have
59 not been well developed. Wang (1981) found that aftershocks caused cyclic shear to induce a
60 decrease in the strength of the sliding surface shear on unstable rock slopes. Some researchers
61 have used inertia, damping, weakening, and liquefied instability to interpret the instability of a
62 deposit. Seed and Martin (1966) used a regular soil deposit for a laboratory test with a limited
63 focus on the large deformation of the inclined slope caused by material liquefaction. Kramer
64 (1997) suggested that postearthquake instability can be spilt into weakened instability and inertial
65 instability. Based on indoor experiments and field tests, a few researchers have studied the
66 liquefaction mechanism and shear deformation of loose deposits after earthquakes in China,
67 Japan, and New Zealand. It was confirmed that liquefaction or shear forces established slope

68 deformation. However, empirical models of the deformation and failure of loose deposits after
69 such earthquakes have not been proposed.

70 According to the survey in 2010 by the China Geological Survey, nearly 45,000 loose deposits
71 were induced by the 2008 Wenchuan Ms 8.0 earthquake in China, extending to 51 disaster areas
72 across 130,000 km². These loose deposits included 13,229 landslide deposits, 5,180 rockfall
73 deposits, and 2,400 debris-flow deposits in Sichuan Province, according to the postearthquake
74 survey (Huang, 2009). Many loose deposits in the Sichuan postearthquake areas are susceptible to
75 rainfall or landslides induced by aftershocks. From 30 May 2008 to 30 December 2010, more
76 than 12,000 potential geological hazards triggered by rainfall and killed hundreds of people (Fig.
77 1) (Kirschbaum, 2010; Liao, 2011).

78 A clear classification system of the deformation mode of the accumulation body is beneficial to
79 the evaluation of the stability of A geohazards. In particular, the geological hazard classification
80 system in strong earthquake areas should consider the effects of multiple factors, such as the
81 topography, stratum lithology, material, motion velocity, deformation, and failure mechanism. A
82 practical type of classification based on selected attributes is a good classification and a quick
83 way to solve practical engineering problems. According to the material and sedimentological
84 characteristics, Fan (2017) divided the dam landslides caused by the 2008 Wenchuan earthquake
85 into three categories, which will help the prevention and control of landslide dams in strong
86 earthquake areas; however, there is no classification for loose deposits such as debris flows and
87 rockfall deposits.

88 In this study, the geological conditions and the type of geohazards induced by the 2008
89 Wenchuan earthquake are first introduced. Subsequently, the classification method and the
90 typical failure mode of the loose deposits that occurred since 2008 are discussed. A new
91 classification method for the deformation and failure modes of deposits considering various
92 factors, such as the topography, material, motion velocity, volume, and particle composition, is
93 proposed. The formation mechanism and failure modes of the geological disasters induced by 12
94 loose deposits are analyzed. The proposed classification scheme of the failure modes for loose
95 deposits could also be easily applied for the classification of geological hazards that occur in
96 other strong earthquake zones.

97 **2. Site Study**

98 **2.1 Geological conditions**

99 Detailed analyses of the landslide deposits show that the slope deposit failures in postearthquake
100 regions in Wenchuan, China, are complex. It is important to study the geological conditions to
101 recognize potential geological hazards. The specific failure mode is related to the specific
102 topography, deformation, and structure of the rock (soil). This study area crosses various
103 geomorphic units covering the Qinghai-Tibet Plateau, Longmen Mountain and the Sichuan Basin
104 and valley from north to south. The elevation is high in the north and west but low in the south
105 and east. Due to well-developed faults, complicated topography, various types of rock-soil mass
106 structures and climate change in this area, many postearthquake loose deposit slopes accumulated
107 in the potential geohazard regions, and it is important to study the failure modes and evolutionary
108 process in the Wenchuan earthquake area.
109

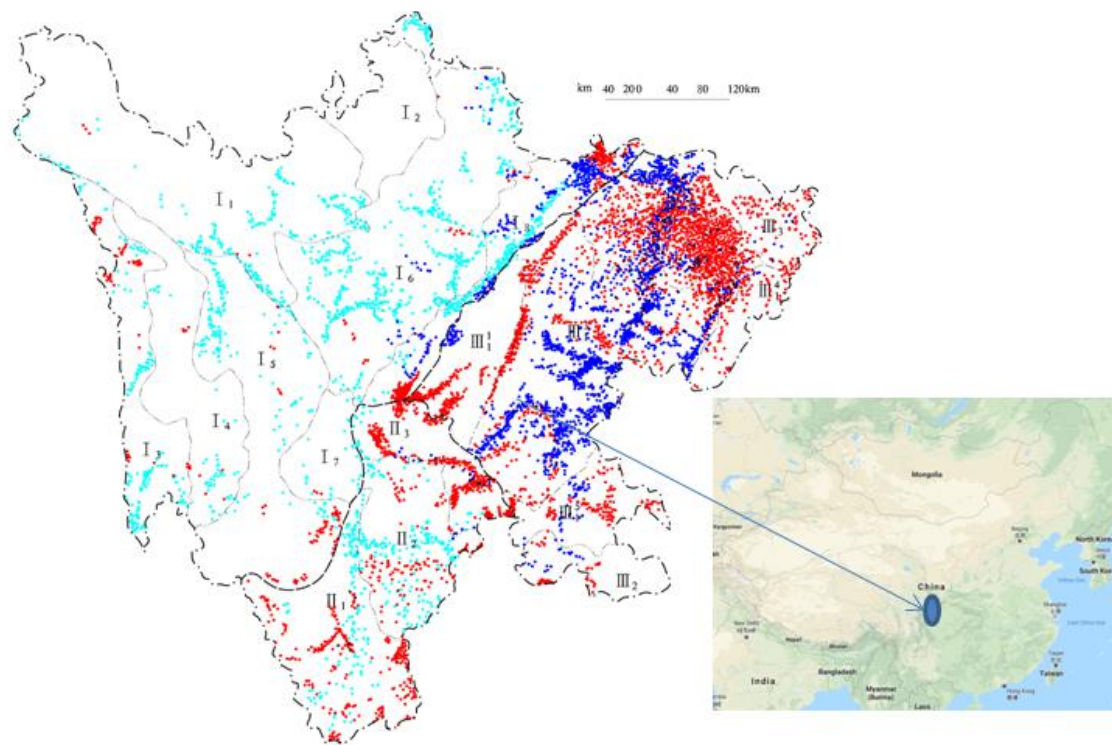


Fig. 1 Statistical distribution of Loose deposits postearthquake in Sichuan Province, China. (Landslide deposits are shown in red; rockfall deposits are shown in blue; debris flow deposits are shown in green. A geological survey in 2010 documented 13,229 landslides, 5,180 rockfalls, and 2,400 debris flows in the study area.)

Legend: ● landslide deposit; ● rockfall deposit; ● debris flow deposit

I: High mountain plateau region of western Sichuan; II: Shiqu Seda structure denuded hilly plateau area; I2: Hongyuan Ruoergai tectonic denuded swampy plains; I3: East bank of Jinsha River tectonic erosion mountain canyon area; I4: Shapuli Mountain erosion or denudation hilly

plateau area; I5: Yalong River structure erodes the deep valley mountain area; I6: Qionlai Mountain to Minshan Mountain tectonic erosion ridge mountains; I7: Gongga Mountain structure erodes extremely high mountains; I8: Longmen Mountain fault erosion slope in the mountain area.

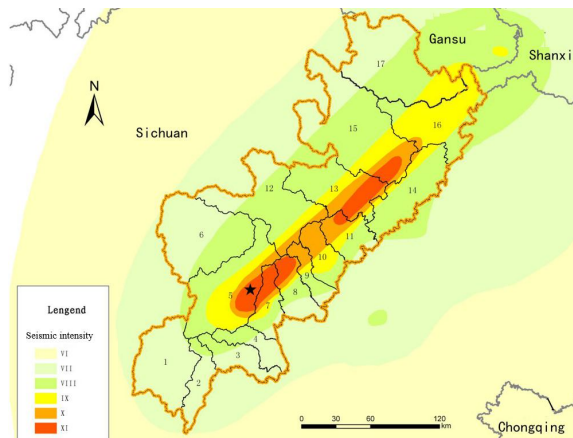
II Mountain area of southwest Sichuan II1: Emei Mountain to Wuzhi Mountain tectonic erosion block mountain area; II2: Xichang Yanyuan tectonics erodes middle mountainous area of wide valley basin; II3: Liangshan tectonic erosion middle mount area.

III: Mountain area in eastern basin in Sichuan; III1: Tectonic erosion low mountain hilly in Sichuan Basin; III₁¹: Inclined plain subregion in the front of western fault depression basin; III₁²: Mono-clinic low mountain subregion north of tectonic erosion basin; III₁³: Table low hilly subregion south of erosion tectonic basin; III₁⁴: Parallelism (low mountain) valley (hilly) subregion in eastern of erosion tectonic basin; III2: Michang Mountain to Dab Mountain tectonic corrosion bedded middle area; III3: Wu Mountain to Dalou Mountain strong karst valley middle mountain area.

110

111 **2.2 Seismicity and rainfall**

112 Several high-magnitude earthquakes have been recorded in the Longmen Mountain tectonic zone
 113 along the eastern margin of the Tibetan Plateau (China) in the last few decades. The Ms 7.5 Diexi
 114 earthquake on August 25 1933, caused a catastrophic landslide that blocked the Minjiang River
 115 and formed three famous “quake lakes”. The rockslide depositions had slipped into a channel and
 116 formed a landslide dam and caused deformation and failure. Subsequently, the water in this lake
 117 poured down and, as a result, 2,500 people were killed and more than 6,800 houses were
 118 destroyed (Ren, 2017). The Wenchuan earthquake on May 12, 2008, and the Lushan earthquake
 119 on April 20, 2013, had magnitudes of Ms 8.0 and Ms 7.0, respectively. These epicenters were
 120 located on the Longmen Mountain fault, SW-NE of Chengdu city, and the epicenter was located
 121 5 to 20 km deep within the Eurasian plate of the Yangtze plate (Fig. 2).



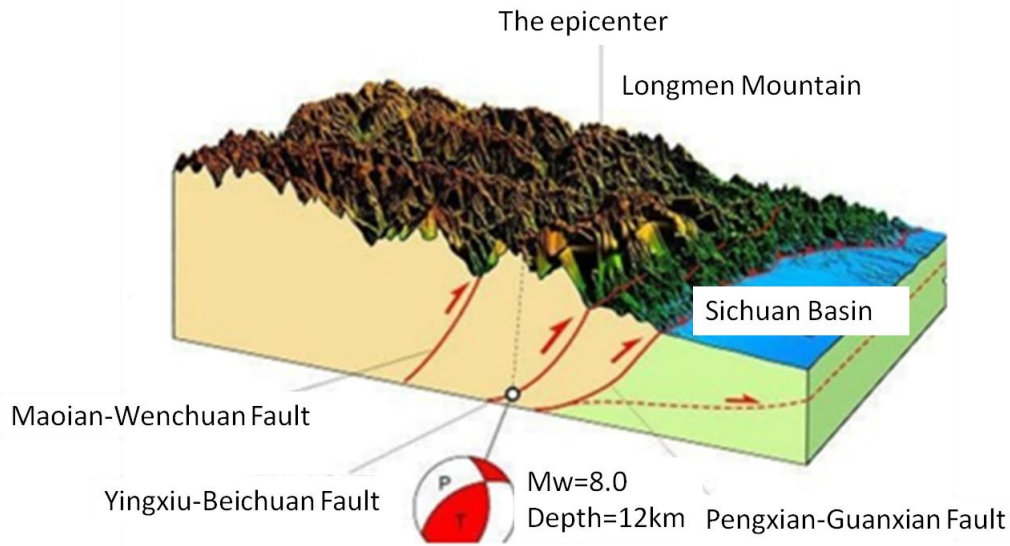
122

123 **Fig. 2 Map of the seismic intensity of the Wenchuan earthquake on May 12, 2008**

124 The abovementioned earthquakes occurred in the Longmenshan fault zone, indicating that strong
125 earthquakes in this area are frequent and that the geological environment is very fragile, which is
126 the source of power for loose accumulations. These recurring earthquakes are the result of the
127 relative uplift of the Tibetan Plateau and the relative decline of the Sichuan Basin. The relative
128 movement of the Qinghai-Tibet Plateau and the Sichuan Basin resulted in the uplift of the
129 Longmen Mountains and formed a large seismic zone parallel to the eastern margin of the
130 Qinghai-Tibet Plateau. The Longmenshan fault zone includes three major fractures, namely, the
131 Maoxian-Wenchuan fault, the Yingxiu-Beichuan fault and the Pengxian-Guanxian fault, which
132 are widely distributed on the two largest anticlinoria: the Pengguan anticlinorium and the
133 Baoxing anticlinorium. Due to the violent new tectonic movement in the area, the rock mass was
134 broken, and earthquakes are frequent, causing a large number of loose deposits (Fig. 3). As
135 shown in Fig. 3, three major faults were formed, i.e., the fault located at the junction of the
136 Longmenshan fault zone and the Sichuan Basin; the piedmont fault, also known as the
137 Pengxian-Guanxian fault, which is approximately parallel to the Longmen Mountains and the 240
138 km main central fault, which is also known as the Yingxiu-Beichuan fault; and the
139 Maoxian-Wenchuan fault, also known as the Maoxian-Wenchuan fault.

140

141 Most typical loose deposits triggered by the earthquake occurred in Longmen Mountain of
142 Wenchuan, which is approximately 60 km from Chengdu city, Sichuan Province, near the eastern
143 fringe of the Tibetan Plateau, China (Fig. 1). Based on the multisource remote sensing data and
144 field survey data from 2009 to 2018 provided by the China Geological Survey (CGS), rainfall is
145 the main cause of the landslides, rock avalanches, and **rotations** caused by loose debris
146 deformation. Among them, the period of 2010-2014 is the peak of the development of rainfall and
147 geohazards, and hundreds of geological disasters were caused by the failure of loose deposits
148 after the 2008 Wenchuan earthquake.



149

150 **Fig. 3 Three main faults along the Longmen Mountain tectonic.**

151 It is suspected that rainfall and aftershocks have triggered landslides or debris flows. Rainfall has
 152 played an important role in the conversion of loose accumulations into landslides and has also
 153 attracted the attention of many research interests. The study area has a subtropical humid climate
 154 that usually brings heavy rainfall between June and September. The average annual precipitation
 155 in the study area is $4.87 \times 10^{12} \text{ m}^3$, and the annual average rainfall is 1003.1 mm. The Longmen
 156 mountain fault zone is in an area of concentrated rainfall distribution with a maximum rainfall of 160
 157 mm in 24 hours, which provides sufficient external dynamic conditions for the failure of loose
 158 accumulations. Besides, there are more than 1,400 rivers in the study area, and the water flow rate
 159 reaches $1.59 \times 10^4 \text{ m}^3$ per second, which is also an important factor for the deformation and failure
 160 of loose deposits (Fig. 4). Under the combined action of seismic activity and hydrogeological
 161 conditions, the slopes with loose accumulations in this area have a high risk of failure during
 162 earthquakes. These factors must be taken into consideration in the failure mode classification of
 163 loose deposits.

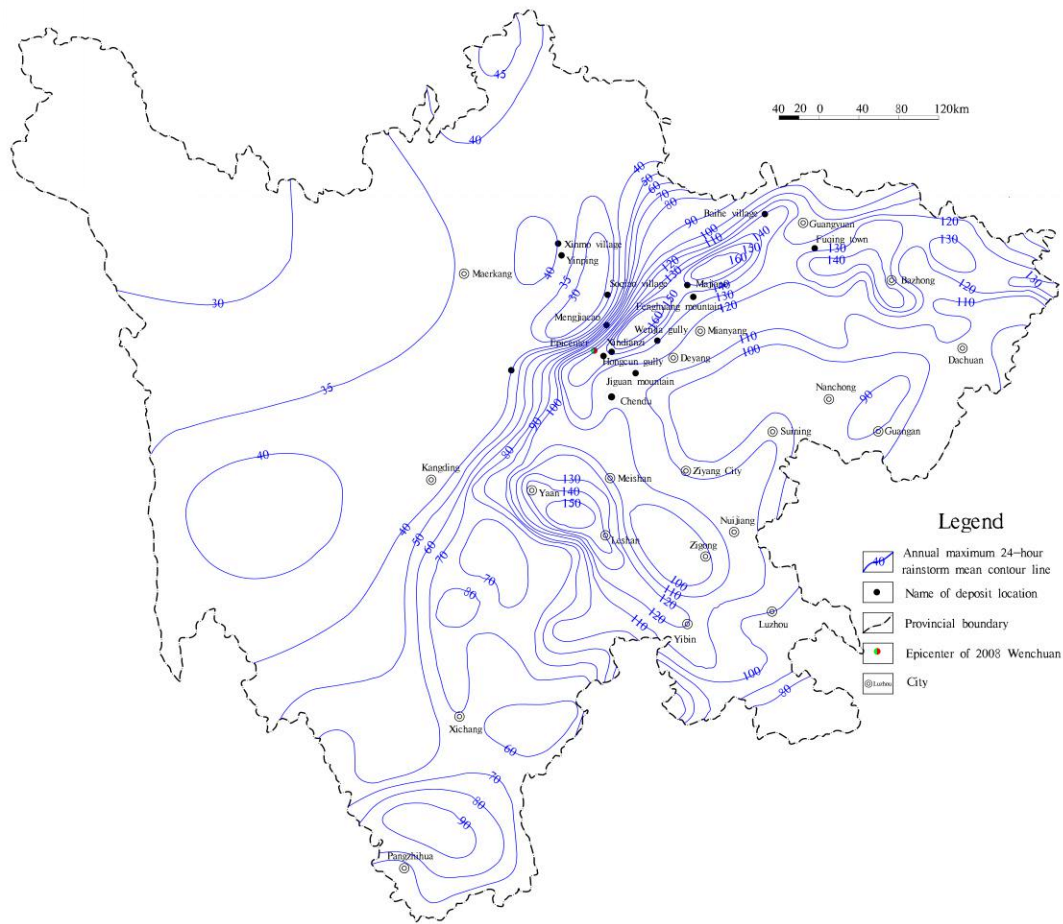


Fig. 4 24-hour rainfall in Sichuan Province

164 **3. Investigation Methods**

165 Field investigations were performed to understand the geological features in the area and the
 166 mechanism of the landslide deposits. The methods include outcrop observations and
 167 topographical measurements, as well as the use of drilling, trenching and pit exploration to
 168 investigate the internal conditions of loose deposits. Geological drilling and standard penetration
 169 testing (SPT) were also used to study the particle composition of some large loose deposits. Due
 170 to the complex and diverse lithology of the landslide loose deposits, the engineering geological
 171 profile of typical loose deposits is drawn based on the investigation and analysis of the lithology
 172 of the strata. Finally, based on a field survey of the representative large loose deposits slopes
 173 along the 50 km-wide Longmen mount fault zone, the deformation and failure mechanisms are
 174 analyzed. (Fig. 4).

175 The field investigation results reveal that the typical lithology of the deposit is bedrock, which
 176 consists of weakly weathered, moderately weathered and strongly weathered coarse and fine
 177 granite, limestone and sandstone. Under weathering or postearthquake weathering, the bedrock is
 178 covered with a large amount of loose clay, broken rock mass or a mixture of the two, which is the
 179 main component of the landslide sediments.

180 According to field investigation statistics for the Wenchuan earthquake area in 2010 (CGS), these
 181 deposits can be classified into four types based on the topography and type of movement (Cruden
 182 and Varnes, 1996), i.e., slide, rockfall, erosion, and debris flow representing 62.74%, 24.57%,
 183 11.38%, and 1.31% of the deposits, respectively. The ratios of slide, rockfall, erosion and flow
 184 types are 41:29.1:28.6:0.4, **respectively**, in the plateau mountain areas. In the high to
 185 medium mountains in a transitional zone from the plateau to the basin, the slide of landslide
 186 deposits induced by the Wenchuan earthquake is the main failure mode (up to 65.3%), followed
 187 by the erosion mode with 26.6%, rockfall type with 6.5%, and debris flow with 1.6%. However,
 188 in the basin and mountain areas in Sichuan Province, the ratios of slide, rockfall, erosion and
 189 debris flow types are 66.9:31.1:0.5:1.5 (Table 1).

190 **Table 1 Category of the landslide deposits in the study area**

Topographic and geomorphic zoning	Type of movement			
	Slide	rockfall	Erosion	Debris flow
Plateau and alpine region	3105	2268	2166	34
High to medium mountain area	2311	231	940	57
Basin and mountain area	8361	3886	65	184
Total number	13777	6385	3171	275

191 **4. Typical failure modes of loose deposits**

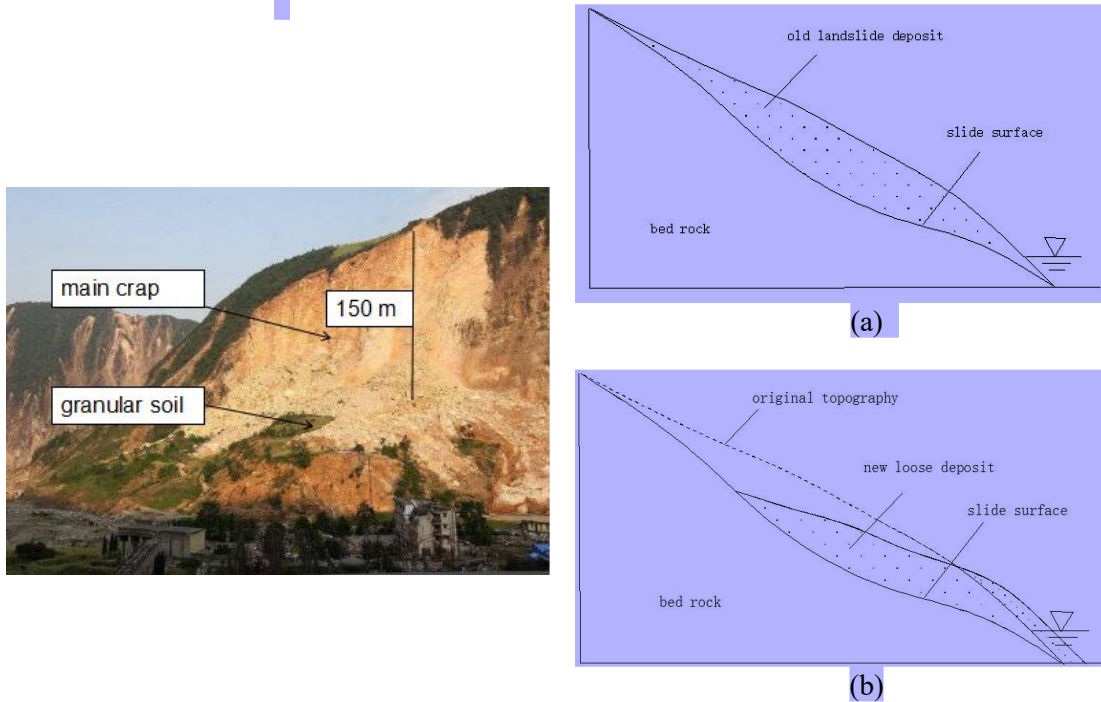
192 **4.1 Slide**

193 The slide type of deposits is usually caused by the reconstruction of rock or soil slopes. Under the
 194 action of external geological forces, e.g., rainfall, aftershocks and human engineering activities,
 195 the loose deposits move along the weak surface or subsurface. According to topography,
 196 materials, motion characteristics, and on-site investigation, we classify the slide into four
 197 categories, including the **rotation of the loose deposit**, sliding along the **weak interlayer**, the
 198 shallow sliding of deep deposits and **translation** on bedding rock.

199 **4.1.1 Rotation of loose deposits**

200 A stable or almost stable ancient landslide deposit body is induced by the earthquake, and
 201 subsequently global or partial **rotation** may occur that leads to deformation and failure of the
 202 accumulation body under the effects of rainfall conditions, aftershocks and human construction
 203 activities. For instance, the Xindianzi landslide, located in Yinxiu town, Wenchuan County,
 204 obviously the epicenter of the 2008 Wenchuan earthquake, is a typical **rotation of loose deposits**

205 (Fig. 5). The source area of the Xindianzi old landslide is nearly 0.8 km long and 0.5 km wide,
206 while the old slope angle is $25^{\circ} \sim 30^{\circ}$. The angle of the old main scarp behind the deposits is
207 steep ($45^{\circ} \sim 75^{\circ}$). The estimated volume of the deposits is $6 \times 10^6 \text{ m}^3$, and the landslide material is
208 a single and homogeneous, mostly loose medium granular soil.



209 **Fig. 5** A slow soil slide on the Xindianzi old landslide: (a) **schematic** of loose deposits before
210 **deformation** and (b) **schematic** of deposits after failure **showing that large homogeneous**
211 **materials stop at the slope foot.**

212
213 The creep and sliding deformation of the Xindianzi old landslide were slow at the beginning, but
214 after the strong rainfall infiltration on August 11, 2010, and the slope excavation on the crown,
215 the landslide displacement and deformation increased rapidly. The water content of this loose soil
216 accumulation increased rapidly after the rainfall, and the gravity of the sliding body also
217 increased. As a result, the shear strength of the main body composed of loose deposits decreased,
218 and even the strength of the soil decreased, resulting in liquefaction. The loose granular structure
219 and high sensitivity to rainwater softening are the basic conditions for the resurrection of ancient
220 landslides, while the most significant localities with **extra sensitive** loose deposits are largely
221 distributed around the Yingxiu-Beichuan main fault zone. A large number of **rotations** of loose
222 deposits have also been found near Mount Tangjia (Hu, 2009)

223 **4.1.2 Slide along with the weak interlayer**

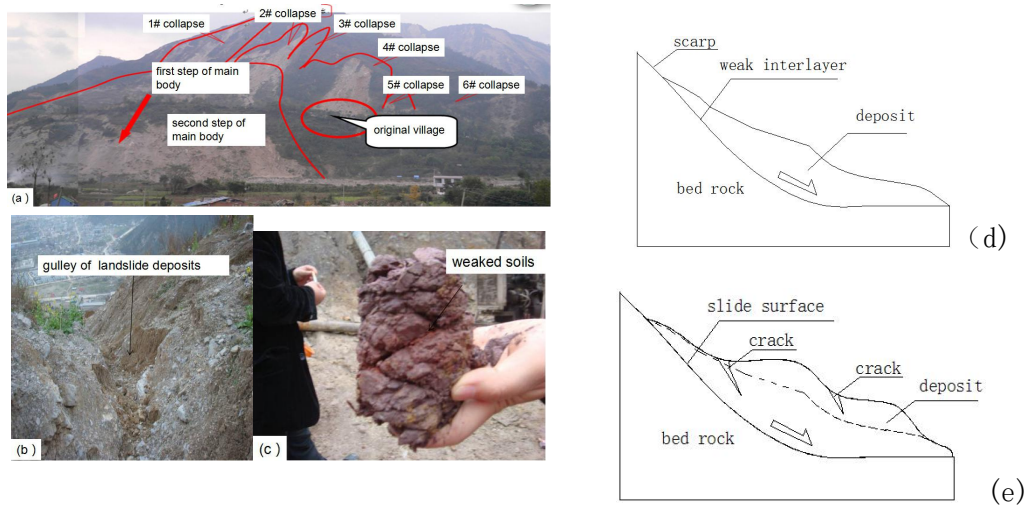


Fig. 6 The landslide that occurred at Fenghuang Mountain, Sichuan, China, in 2011: (a) image of Fenghuang Mountain landslide; (b) Gully at the trailing edge of a landslide; (c) soft crushed soil from drilling; (d) Schematic of loose deposits before failure; and (e) Schematic of loose deposits after failure.

224

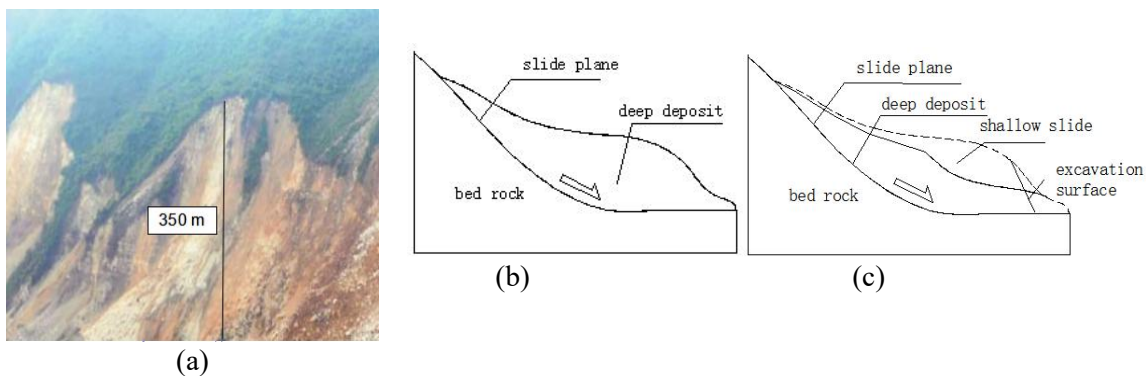
225 Slides along with the weak interlayer usually occur in deposits with weak substrate. The main
 226 body consists of loose deposits, broken rocks, and their mixtures. The weak interlayer consists of
 227 plastic-soft clay or clastic sediments, and the bedrock usually consists of fully weathered-
 228 weathered shale, mudstone or sandstone. Before the deformation of the rock and soil in the weak
 229 interlayer occurs, the landslide generally moves slowly, and the moving speed is usually less than
 230 0.1 m/a. However, under the influence of earthquakes, rainfall and human engineering activities,
 231 the loose deposit will suddenly accelerate in the case of the transfixion of a weak interlayer or a
 232 weak zone (Huang, 2011).

233 The Fenghuang Mountain landslide is located in Ershe village, Leigu town, Beichuan County,
 234 with a total volume of approximately $1.08 \times 10^6 \text{ m}^3$; it is a slide on a weak interlayer, and the
 235 landslide deposit is nearly 420 m long and 1560 m wide, with an average slope angle of 25° ,
 236 which is affected by deformation. The main scarp is 25 m high on average, presenting two
 237 moving steps, with a horizontal distance of 167 m and a height of 80 m. The middle of the deposit
 238 is 111.6 m thick, 94 m thick at the slope toe and 58 m thick at the slope head. Most of the
 239 material in this landslide deposit is composed of limestone, carbonaceous shale, silty clay,
 240 crushed stone or pebbly clay. The soil sample exposed by drilling is characterized by kneading
 241 and water absorption, suggesting that the soil sample is subjected to high compression and
 242 grinding. According to geological hazard monitoring, the slip velocity of this accumulation body

243 is 0.08 m/year. Excavation of the road at the toe of the slope resulted in the rapid downward
244 movement of the deposit along the weak interlayer (Fig. 6).

245 4.1.3 Shallow slide of deep deposits

246 A shallow slide on deep earthquake deposits generally occurs in highly consolidated deep rock
247 and soil. The velocity is extremely high (often greater than 0.1 m/a), and sometimes the surface
248 fragmentation of the soil accelerates as the slope increases throughout the movement. This type of
249 failure is caused by earthquakes, rainfall or human activities and leads to the deterioration of the
250 structure and strength of the shallow surface of the stratum, followed by the creep and sliding
251 deformation of the shallow part of the deposit body (Fig. 7).



252 **Fig. 7 Majiapo landslide in Beichuan County: (a) photograph of a shallow slide in the**
253 **Majiapo shallow landslide, Sichuan Province, China; (b) schematic before failure; and (c)**
254 **schematic after failure.**

253 The Majiapo landslide, which is nearly 330 m wide and 230 m long, is located in Yuli town,
254 Beichuan County. The landslide volume is nearly $4 \times 10^5 \text{ m}^3$, and the main body is less than 10 m
255 thick. The landslide deformation was very slow before the Mount Tangjia earthquake lake was
256 formed. However, after the toe of these deposits was submerged by the water, the shallow
257 landslide moved quickly. The landslide deposits have a steep ($25^\circ \sim 45^\circ$) slope angle
258 approximately 28 m high. The composition of the deposits is largely gravelly soils with highly
259 weathered phyllite and slate (50-60%). Likewise, these shallow landslides are known to occur
260 both on the surface land and under the earthquake lake water.

261 4.1.4 Translation on bedding rock

262 Translation on bedding rock generally occurs in loose rock deposits with a forward gentle laminar
263 rock layer. The topography of this failure mode is characteristic of V-shaped or U-shaped valleys.
264 These slopes are composed of medium-to-sloping layered rocks. They may slide along the

265 bedding plane under the action of their weight or load, or they may incur deformation and failure
266 caused by external loads, such as rainfall or earthquakes.

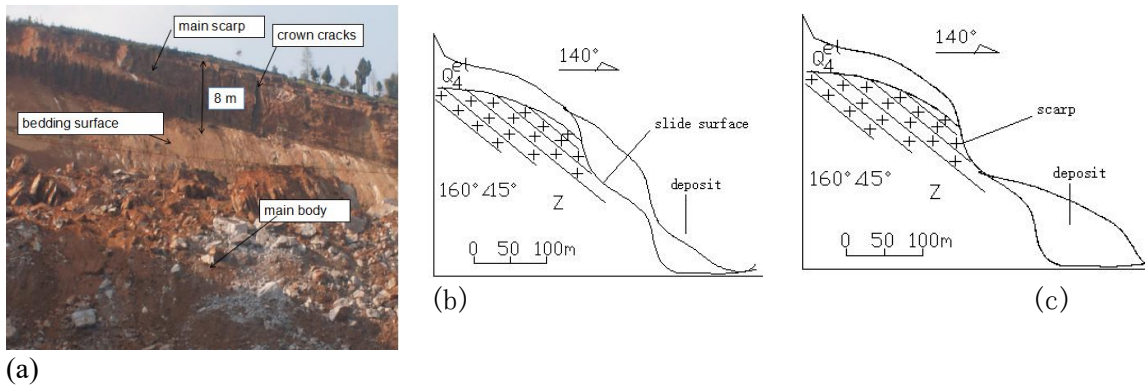


Fig. 8 Photograph and schematic of a slide in Fuqing town, Wangchang County, Sichuan Province, China, in 2011.

267

268 A **translational** landslide is located in Fuqing town, Wangchang county, Sichuan Province. The
269 landslide was formed during the 2008 Wenchuan earthquake, and the tectonic crown cracks were
270 0.5-1.0 cm wide and 1-2 m long or 0.5-0.8 cm wide and 2-3 m long. The landslide, **with a deposit**
271 **area of $1.36 \times 10^4 \text{ m}^2$ and a total volume of $1.31 \times 10^5 \text{ m}^3$** , occurred after constant rain in July 2011.
272 The formation lithology in the landslide deposit primarily consists of sandstone of the Triassic
273 system (*T*) and Quaternary residual slope alluvial soil (*Q*). The angle of the bedding rock is steep
274 (more than 35°), and the main body is 9.6 m high on average, of which the main scarp is 8 m in
275 height. The remaining unstable landslide height of 8 m may slide suddenly in the future.
276 According to field reconnaissance, the velocity of this landslide is 0.5 m/year, and rainfall
277 infiltration and a weak surface along the bedding limestone are the main failure factors (Fig. 7).

278 4.2 Rockfall

279 Rockfall is produced in steep slope deposits under external forces, including gravity, earthquakes,
280 weathering denudation or human activities. It is a single or compound movement with sharp fall,
281 caving, sliding, rolling, jumping, and other special forms; sometimes **rocks** hit each other in the
282 process of movement **and** then pile at the slope toe (Rens, 2008). Most of the rockfall sources are
283 rock deposits with low shear strength and 2-3 groups of penetrating fractures. Whether rockfall
284 occurs depends on the deposit steepness and deposit stability. Based on the rockfall travel
285 velocity and movement method, the rockfall type can be split into the following three subtypes.

286 **4.2.1 Rockfall slide**

287 **The** Xinmo catastrophic rockfall sliding avalanche is a recently famous massive rockfall in the
288 Wenchuan earthquake area, with 10 deaths and 73 people missing. These massive deposits are
289 located in Xinmo village, Diexi town, Mao County, Sichuan Province. This event may have
290 originated from the 1993 Diexi Ms 7.3 earthquake, which caused several cracks in the crown of
291 the slope. Besides, after a long period of weathering, rain erosion, and the 2008 Wenchuan Ms
292 8.0 earthquake, the trailing edge fissure on the slope stretched downward and finally passed, and
293 then the massive rock mass traveled more than 2 km. The total volume of the rock mass deposit is
294 approximately $4.5 \times 10^6 \text{ m}^3$, it is approximately 210 m long and 300 m wide, and the fastest
295 traveling velocity of the massive loose landslide deposit is approximately 74.6 m/s (Fig. 9) (Xu,
296 2017; Fang, 2017; Meng, 2018).

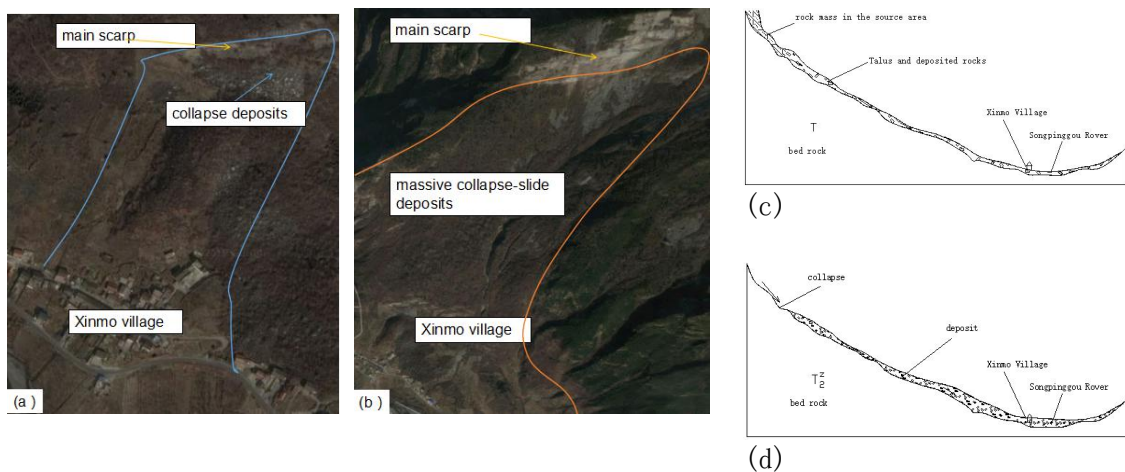


Fig. 9 Photograph and schematic of the massive rockfall in Xinmo village, Diexi town, Sichuan, China, in 2017: (a) photograph of the rockfall deposits on May 10, 2017; (b) photograph of the massive rockfall-slide deposits on May 20, 2018; (c) schematic of the massive deposit before failure; and (d) schematic of the massive deposit after failure.

297
298 Massive rockfall-sliding is one of the catastrophic disasters that pose threats to people's lives in
299 earthquake areas. If the loose deposits consisted of densely structured rocks and joint fissures that
300 had an unstable effect on the rocks that were extensively distributed, fractures would be formed
301 through a plane. Subsequently, under the action of multiple earthquakes and long-term gravity,
302 aging deformation is generated. Under the continuous rainfall infiltration, the water level in the
303 loose accumulation body continues to rise, and the anti-slip force decreases., the stability of the
304 loose deposits slope decreases, and a catastrophic landslide may occur suddenly.

305 **4.2.2 Crack-slide rockfall**

306 A crack-slide rockfall is a form of a steep slope characterized by steep and vertical fractures on
307 the crown of the slope, occurring when loosely cemented material or rock layers move a short
308 distance and dump at the toe of the slope (Tarbuck, 1998). Although the surface of the slope
309 displacement is small, deep crown cracks are formed by rain infiltration, earthquakes, or
310 weathering (Fig. 10). Moreover, the gravity of overburden deposits based on the weak layer
311 increases in the process of rainfall, thereby causing deposits to fall gradually along a parallel
312 surface. This deformation mostly occurs in the consequent bedding landslide deposits.

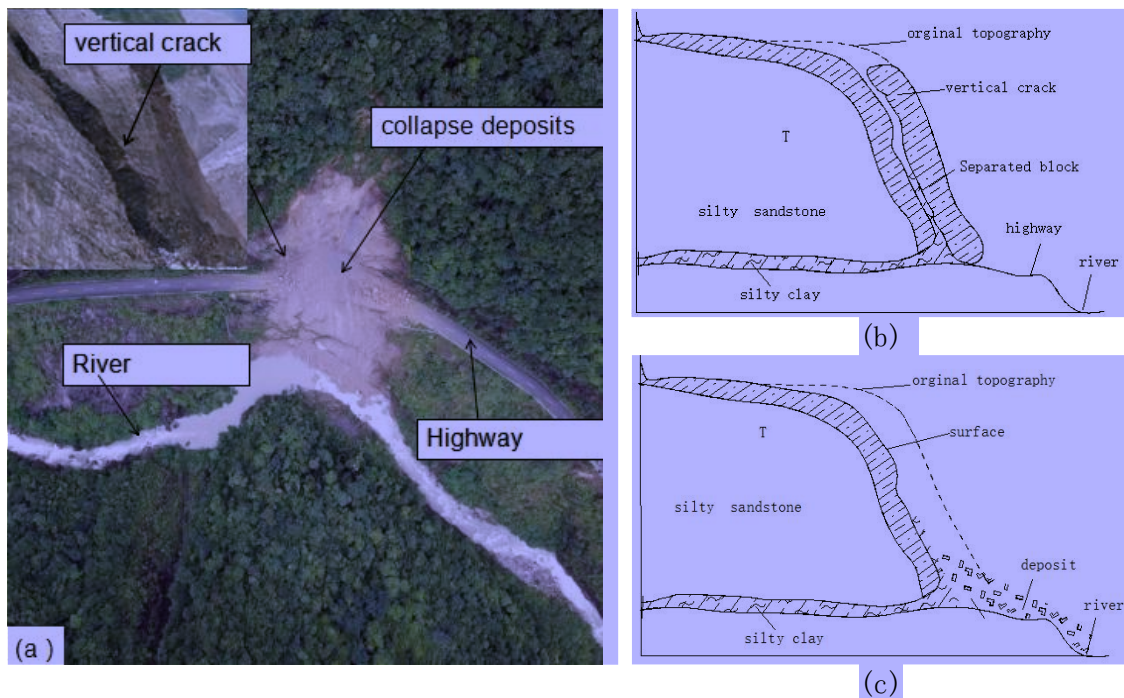


Fig. 10 Aerial photograph and schematic of crack-slide rockfall in Jiguan Mountain, Chongzhou city, Sichuan, China, in 2018: (a) aerial photograph of Jiguan Mountain; (b) schematic of loose deposits before failure; and (c) schematic of the crack-slide rockfall.

313
314 The Jiguan Mountain crack-slide rockfall, which is approximately 40 km south of the epicenter of
315 the 2008 Wenchuan earthquake, occurred on July 9, 2018. Fig. 10 shows an aerial photograph of
316 the rockfall. At the crown of the rockfall, there were several vertical cracks approximately 2.5 m
317 deep. The rockfall deposits were approximately 250 m wide and 560 m long with a total volume
318 of approximately $3.8 \times 10^6 \text{ m}^3$. Most of the materials in the deposit were primarily composed of
319 silty sandstone and limestone that formed in the Triassic period of the Mesozoic era. In the area
320 where the rockfall occurred, the artificial slope was 7.5 m high with an angle of over 70° and
321 covering considerable underlying rocks on the consequent bedding sandstone layer.

322 **4.2.3 Toppling rockfall**

323 Toppling failure is one of the most common failure forms of rock deposit slopes in strong
324 earthquake areas. The main failure mode of the toppling failure is bending and overturning, which
325 is caused by bending stress. Toppling generally occurs in steep rocks with vertical joints.
326 Moreover, soft rock and hard rock **interbedded** sedimentary strata often undergo toppling failure.
327 When the lower soft interlayer is weathered or eroded by rainfall, the upper loose accumulation
328 body is suspended, falls and rebounds or rolls downhill under the action of gravity. Toppling
329 rockfall is characterized by breaking rocks and discontinuous structural cracks, usually triggered
330 by earthquakes or human activities (e.g., hydropower station building, highway building, and
331 other works) (Guo, 2017). In addition, effective intergranular stress would decrease in the
332 deposited material due to the increase in internal seepage pressure and the decrease in pore water
333 pressure, thereby causing a rockfall. This deformation failure model can be defined as toppling
334 rockfall.

335

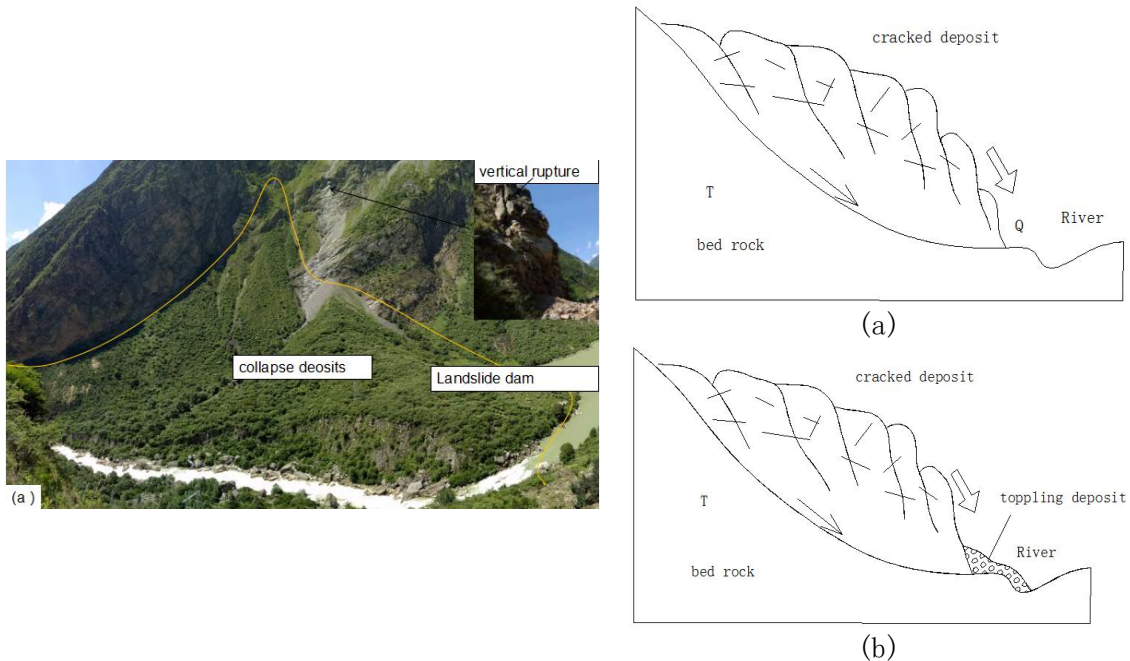


Fig. 11 Aerial photograph and schematic of toppling rockfall at Yinping, Mao County, Sichuan, China: (a) aerial photograph at Yinping; (b) schematic of toppling rockfall before failure; and (c) schematic of toppling rockfall after failure.

336

337 For instance, the Yinping toppling rockfall was triggered by the 1933 Diexi Ms 7.3 earthquake
338 and the 2008 Wenchuan earthquake. **These** rockfall deposits formed from 1993 and blocked the
339 Min River. The geostructure of this landslide dam is featured by the consequent bedding structure
340 and cliff. Because the rock has been falling for 85 years, the rockfall deposits are approximately

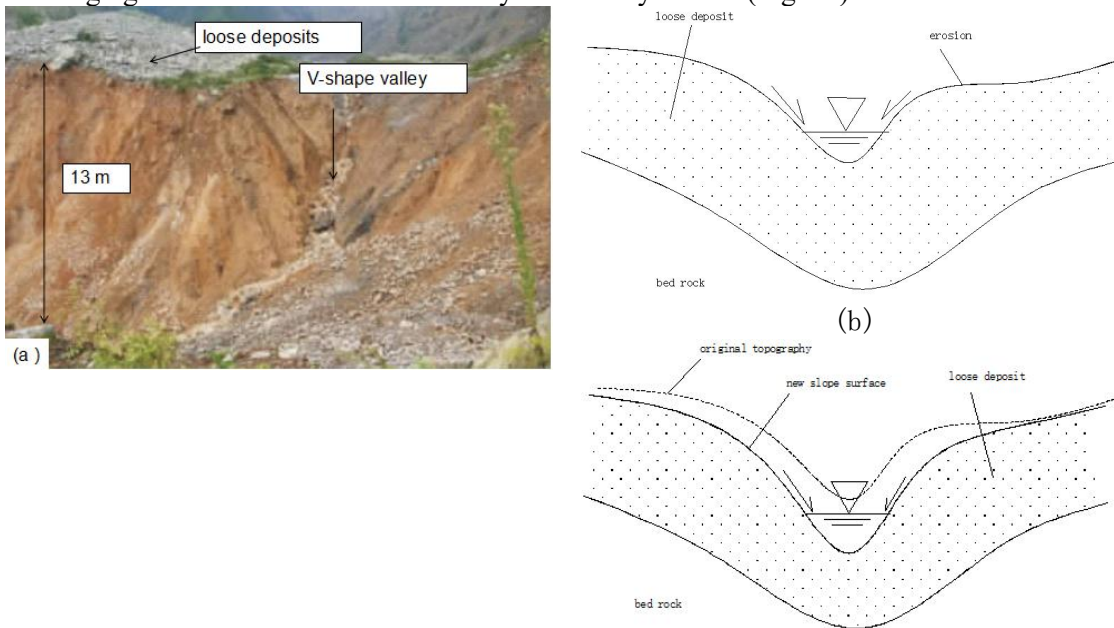
341 1000 m wide and 1500 m long, and the rockfall rock travels a distance of more than 1400 m
342 (Huang, 2009). After the 2008 Wenchuan earthquake, the average thickness of the rockfall
343 deposits was over 180 m, and the total volume was over $2.1 \times 10^8 \text{ m}^3$. The stratigraphic lithology
344 of such landslides is generally composed of quaternary (Q) residual slope sediments, Triassic
345 metamorphic rocks and crystalline limestone (T).(Fig. 11).

346 4.3 Erosion

347 Erosion often occurs in loose deposit bodies induced by rainfall or flow in areas with undulating
348 landscapes. This mode of motion is usually a spatially continuous motion, and the deposit is
349 carried away by the current from high to low elevations. These processes contribute to the
350 formation of unstable rock and soil masses on the surface of gullies during different courses of
351 geological erosion (J. Dvorak, 1994), deformation and destruction, and the deposits finally move
352 with the grading movement of mud (sand) flow, which depends on the water content, mobility
353 and movement evolution.

354 4.3.1 Sheet erosion

355 Sheet erosion has two main mechanisms: scouring and lateral erosion. River erosion is the direct
356 removal of soil particles by the current. The rate of scouring is determined by the impact of the
357 flow and the erosion resistance of the bank's loose deposit material. When the weight of the upper
358 deposit is greater than the strength of the slip zone, the failure will occur subsequently, resulting
359 in lateral erosion. The process depends on many factors, including the particle composition of the
360 slope material, the water content and the coverage by vegetation. These two erosion processes are
361 interrelated because the scouring at the bottom of the riverbank produces steeper slopes or
362 overhanging clods that are unstable and may be laterally eroded (Fig. 12).



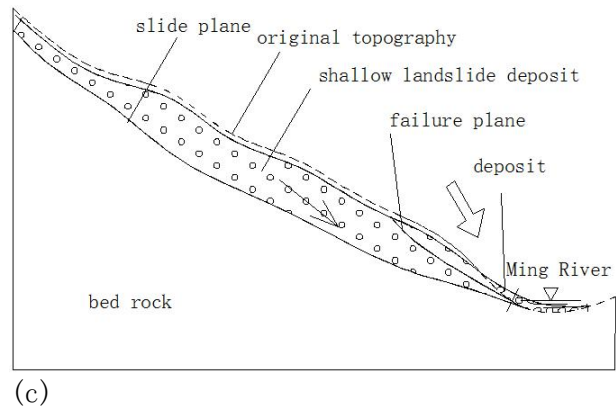


Fig. 13 Schematic and photograph of bank erosion in Rope bridge/Soqiao village, Wenchuan County, Sichuan Province, China, in 2014: (a) photograph of gully erosion of the bank deposit; (b) schematic of deposits before the failure; and (c) schematic of deposits after the failure.

382

383 Streambank erosion in Suoqiao village is located on the left bank of the Minjiang River, which
 384 has a middle mountain canyon landform. The deposit is approximately 200 m wide and 220-250
 385 m long, while the main body area is approximately $3.88 \times 10^4 \text{ m}^2$ with a total volume of 6.52×10^5
 386 m^3 . Most of the material in the toe is gravelly soil, including 10%~30% phyllite and limestone
 387 debris. The movement of the eroding bank is slow in winter, but the loose deposits move faster in
 388 the rainy season. The Suoqiao deposits are unstable because of the bank erosion at the toe, and it
 389 has a weak sliding surface. Accordingly, landslides are expected to occur in future heavy rain or
 390 earthquake conditions.

391 4.3.3 Debris flow cutting

392 Debris flow cutting typically occurs on a slope of loose deposits with a slope up to 45° and is
 393 usually initiated during heavy rainfall, with upstream materials driven by a rainstorm or debris
 394 flow. When the water accumulates rapidly upstream, a debris flow will form in the middle and
 395 lower reaches, subsequently rushing out of the channel, and cutting the slope foot, which results
 396 in a steep exposed surface. The existence of these loose materials on the slope and the
 397 development of heavy rainfall events are the main reasons for the deformation and failure of these
 398 deposits (Xu, 2012).

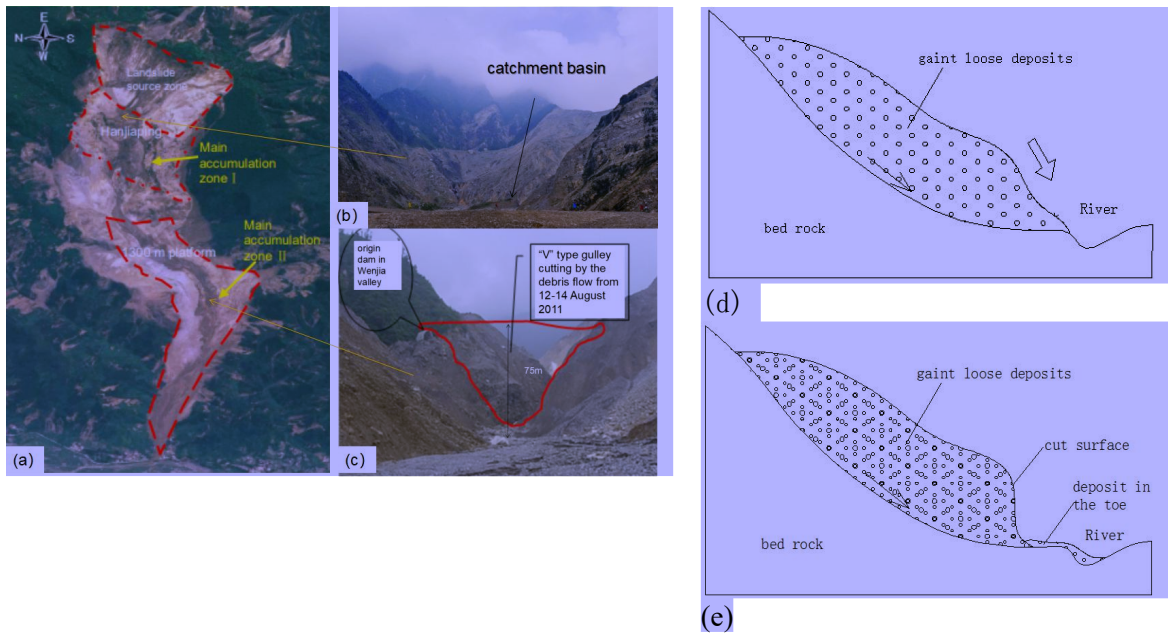


Fig. 14 Schematic and photograph of debris flow cutting in Wenjia gully, Qingping town, Sichuan Province, China, in 2010: (a) aerial photograph of Wenjiagou deposits; (b) photograph of upstream debris flow deposits; (c) photograph downstream of the Wenjiagou debris flow deposits; (d) schematic of the deposits before the failure; and (e) schematic of the deposits after the failure.

399

400 The famous debris flow cutting type is in Wenjia gully, which is located north of Qingping town,
 401 Mianzhu city, Sichuan Province, China. The catastrophic deposits were formed by the 2008
 402 Wenchuan earthquake and have experienced several events of heavy rain and continuous rain.
 403 From September 2008 to September 2011, six large-scale debris flows were formed, which
 404 seriously endangers the safety of life and property downstream. The accumulation body has a
 405 relative height difference of 1.49 km and a ditch length of 4.9 km, and the overall slope dropped
 406 by 306%. The profile of the accumulation body shows three-level platform accumulation with the
 407 upper slope, middle and lower level. The trailing edge and the leading edge of the accumulation
 408 body of Hanjiaping, the first-level platform, are both steep (the gradients are 673.8‰ and 644.4
 409 ‰, respectively), which significantly contributes to the formation of the catchment power
 410 accelerating the discharge. The slope falls of the secondary platform (1300 m) and the tertiary
 411 platform is relatively small (140.3‰ and 322.5‰, respectively), whereas the ditch is deep and
 412 narrow and the accumulation body exhibits a large loose thickness, which makes it extremely
 413 easy for erosion and erosion cutting deformation and failure.

414 4.4 Flow

415 **4.4.1 Rock avalanche**

416 The **rock** avalanche originated from collapsing material caused by the earthquake. Because of the
417 steep slope, scarce vegetation and extremely loose structure of the deposit, combined with
418 exterior geological forces (e.g., aftershocks and human activities), debris flow material in a
419 superficial layer of loose deposits slipped downward with high speed, accompanied by the
420 flow of dust and the sounds of tumbling rocks.

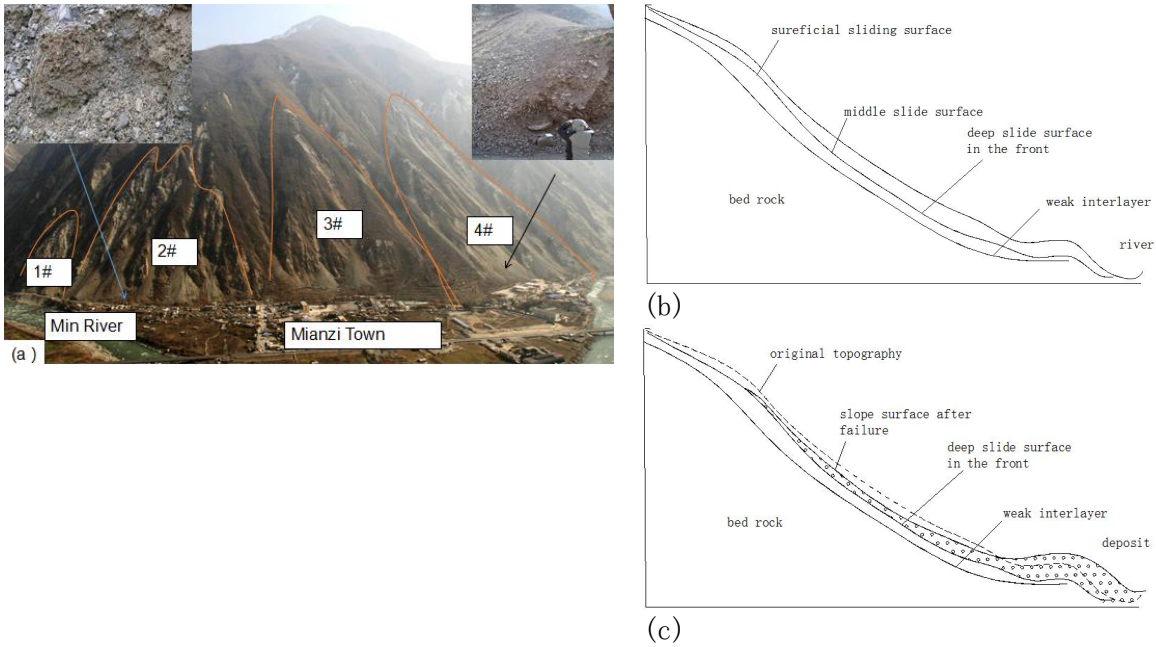


Fig. 15 Photograph and schematic of the **rock** avalanche at Mengjiacao, Mianzi town, Wenchuan, Sichuan, China: (a) photograph at Mengjiacao; (b) schematic of toppling rockfall before failure; and (c) schematic of toppling rockfall after failure.

421
422 Since 2008, there have been hundreds of **rock avalanches** induced by rainfall or aftershocks in the
423 Wenchuan earthquake area. The speed of the avalanche chute to the steep channel is usually more
424 than 10 m/s, whereas some of the landslide flows are much faster. For instance, the Mengjiacao
425 **rock avalanches**, located in Mianzi town, approximately 10 km south of Wenchuan County,
426 Sichuan Province, are typical avalanche flows in this area. Because of the rockfall flow since
427 2008, the rock or soil has accumulated at the toe of the slope, and the total volume of these
428 deposits is over $2.5 \times 10^6 \text{ m}^3$. The materials of **these** landslide-debris flows contain characteristics
429 of the loose coarse and fine particles that are distributed in the different rockfall areas. The
430 landslide debris in the steep channels usually attains speeds of over 12 m/s (Fig. 15).

431 **4.4.2 Debris flow**

432 Although the number of mudslides in the Wenchuan earthquake area is only a small proportion,
 433 accounting for about 1.31% of the total number of mudslides in the country. But because of the
 434 loose deposits, mudslides occur more frequently in the region than in other parts of China,
 435 attracting a lot of attention from engineers and the government.. For instance, the Hongchun gully
 436 debris flow occurred near Yinxiu town, Wenchuan County, Sichuan, on August 14, 2010,
 437 resulting in 17 missing persons. The debris flow has battered the new 213 National Highway,
 438 blocked the Min River, and then destroyed Yinxiu town (Fig. 16).

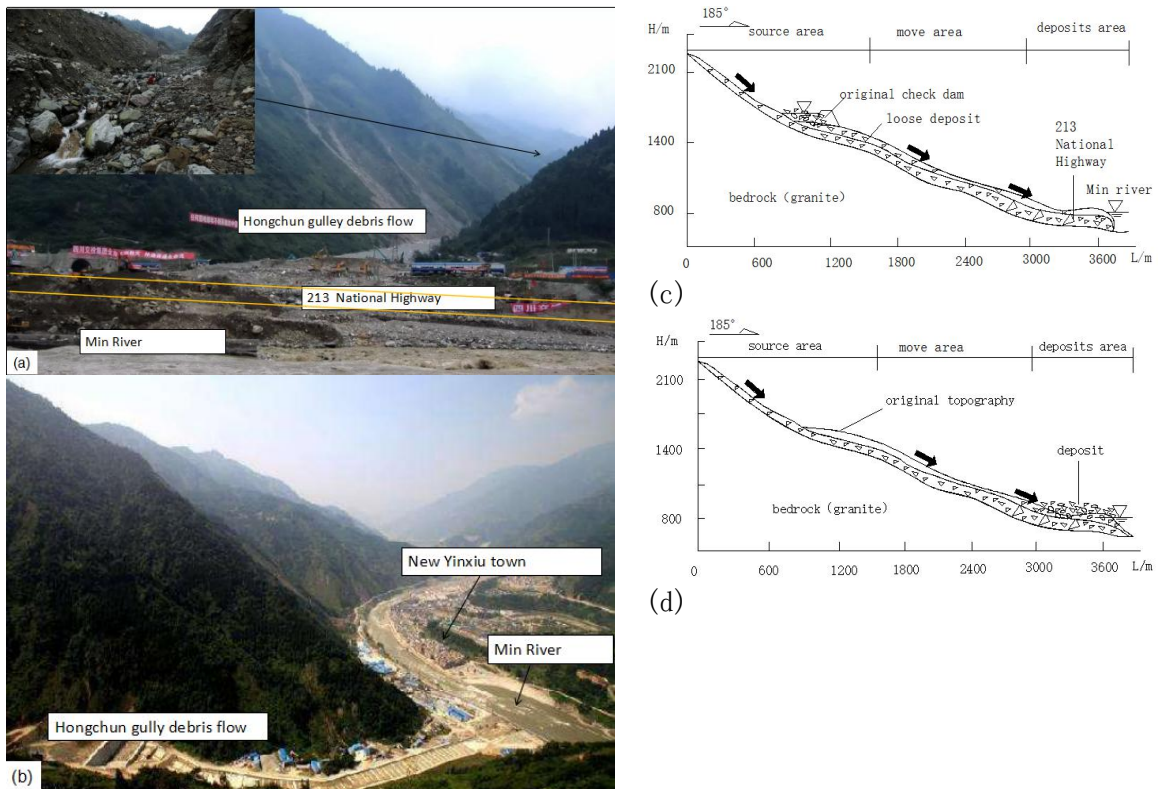


Fig. 16 Photograph and schematic of debris flow at Hongchun gully, Yinxiu town, Wenchuan, Sichuan, China: (a) photograph at Hongchun gully in 2009; (b) image of Hongchun gully in 2018; (c) schematic of debris flow before failure; and (d) schematic of debris flow after failure.

439

440 The Hongchun gully debris flow is one of the 72 debris flows near the Beichuan-Yinxiu fault in
 441 August 2010, which is characterized by the number of loose deposits, the steep drop in the shape
 442 of the gullies and critical rainfall (Tang, 2009). The total volume of this debris flow is nearly 80.5
 443 $\times 10^4$ m^3 , and all of the loose materials of the debris flow are composed of granular soil (60%),
 444 boulders (25%), rubble (10%) and sand (5%). The channel catchment area covers 3.35 km^2 , the
 445 main channel length is 3.6 km , and the average longitudinal slope of the channel reaches 35.8% .
 446 The top of the slope is 2168.4 m asl, and the gully mouth of debris flow is at 700 m asl. The

447 debris flow materials mainly come from three branches in the upper reach of the Hongchun gully,
 448 among which 52% are landslide or rockfall deposits, and the total amount of loose solid material
 449 is 3.57×10^6 m³. Moreover, because the rainfall prior to the “8.14” debris flow outbreak in
 450 Hongcun gully was 16.4 mm per hour and the total rainfall reached 162.1 mm in 34 hours, heavy
 451 rainfall was the inducing factor of the debris flow outbreak (Gan, 2012).

452 5 Discussion

453 Previous studies have suggested that different types of accumulation slopes have significantly
 454 different deformation and destruction mechanisms and failure modes (Zhang, 2012; Cui, 2014;
 455 Huang, 2015). Controlled by various factors (e.g., rock and soil mass structure, geological
 456 structure, rainfall, and geography and geomorphology) of the study area, the accumulation body
 457 presents different deformation and failure modes, and its movement type, speed, scale,
 458 geomorphology, landform and failure modes are also different (Table 2).

459

460 **Table 2 Table of characteristics of deformation and failure of loose deposits in the**
 461 **Wenchuan earthquake area**

Failure type of landslide deposits	Topography	Material	Travel velocity	Volume	Triggering mechanism	
slide	Rotation of the loose deposit	Mountain, Hill, Talus	Gravel, Sand, Clay, limestone	Various	Small to Large	Rainfall, Earthquake, Human activities
	Slide on weak interlayer	Mountain, Hill	Weak rock, Gravel, Sand, Silt	Slow	Large	Rainfall, Earthquake, Human activities
	Shallow slide of deep deposits	Mountain, Hill or Valley Talus,	Gravelly soils, Weathered rock, Consolidated Soils, Rocks	Slow to Ex. Rapid	Small	Earthquake, Weather, Human activities
	Translation on bedding rock	Mountain		Slow	Large	Earthquake, Rainfall, Human activities
rockfall	Rockfall-slide	Mountain	Rock, Soil	Rapid	Small to Large	Weathering, Rainfall, Earthquake
	Cracking sliding of rock rockfall	Mountain, Hill	Rock	Slow to Ex. Rapid	Small, Middle	Weathering, Rainfall, Earthquake
	Toppling rockfall	Steep Cliff	Rock	Rapid	Small to Large	Weathering, Rainfall, Earthquake

erosio n	Sheet erosion	Valley, Gully	Loose Soil or Clay, rock deposits	Slow	Small to Large	Rainfall, Weather,
	Gully erosion	Valley, Gully, River	Soils, Sand, Silt	Slow to Ex. Rapid	Small to Large	Rainfall, Weather
	Debris flow cutting	Valley, Gully	Rock, Sand	Ex. Rapid	Middle, Large	Rainfall, Weather
flow	Rock avalanche	Mountain	Rock, Clay	Slow to Rapid	Small, Middle	Earthquake, Weather, Rainfall, Rainfall
	Debris flow	Mountain , Hill, Valley	Stone, Soil, Sandy gravel	Ex. Rapid	Middle, Large	

462

463 It is worth noting that topography is a factor that significantly affects the failure of landslide
464 deposits. It also determines the scale, shape and deformation and destruction mode of these
465 accumulation slopes. Macroscopic topography controls the development and distribution of
466 deposit bodies. Slopes with different gradients, heights, shapes and vegetation significantly affect
467 the disaster mode of landslide deposits.

468 There was no clear relationship between the failure mode of the deposits and [the observed](#)
469 particle sizes. Deposits are composed of fine-particle soil (e.g., sandy soil, gravel soil, and clay)
470 that can cause sliding, erosion and debris flows. Deposits composed of medium and coarse
471 particles can also fail as long as there is sufficient rainfall. The precipitation process of the
472 rainfall intensity significantly affects the formation of debris flows. This study suggests that
473 continuous rainfall and rainstorms can lead to different failure modes through the same deposits
474 with the same particle sizes. Vegetation and its root system can [lessen erosion](#) and protect the
475 deposits from being eroded by rainwater. Investigations reveal that deposits with well-developed
476 vegetation primarily form slip-type deformation and destruction, and it is unlikely to develop into
477 erosion or rockfall. In contrast, rockfall or erosion deformation and destruction often occur in
478 places with poor development or underdeveloped vegetation in landslide deposits.

479 Moreover, the formation of accumulations was controlled by geological structure. The closer the
480 distance to the Longmen [Mountain](#) seismic fracture zone, the greater the seismic forces, and the
481 structure of the accumulation [becomes](#) loose to form debris flows, which may likely be
482 transformed into the rockfall type and erosion if the landslide deposit produced is much closer to
483 the fracture zone. Investigations reveal that the failure of landslide deposits in the Wenchuan
484 earthquake area was primarily developed in rock and rock-soil (e.g., granite, quartzite, dolomite,
485 and limestone). [Translation](#) on bedding rock mostly occurred in rock deposits composed of hard

486 rock at the top and weak rock at the bottom. Deposits are largely composed of rocks at the top
487 with a highly compacted density and weak structural bedding surface, thereby easily inducing a
488 slide on a weak interlayer. Most giant landslide deposits are located on the steep slopes near the
489 Longmen Mountain fault belt, and it is extremely easy to produce catastrophic landslides or
490 debris flows.

491 **6 Conclusions**

492 Previous classification studies on loose deposits were based primarily on the material, velocity,
493 water content, geotechnical parameters, and other geological hazards, and the effects of
494 topography, landform, volume, and triggering mechanisms were generally not considered. This
495 paper presented a world-recognized classification improvement from the perspectives of the
496 topography, velocity, material, volume and triggering mechanism of loose deposits in a strong
497 earthquake area. Thus, the basis of these factors in this classification is comprehensive and
498 especially suitable for the actual classification of geological disasters in the meizoseismal area,
499 which helps provide a scientific basis for the prevention and control of geological disasters.

500 According to the results of field investigations and statistical analysis, there were four main types
501 and 12 subcategories of failure modes in the loose deposits after the 2008 Ms 8.0 Wenchuan
502 earthquake area as follows: (1) [slide, including rotation of the old deposits, slide along the](#)
503 [interlayer](#), shallow sliding of deep deposits and translation on bedding rock; (2) rockfall,
504 including rockfall-slide, cracking-sliding rock rockfall, topping soil rockfall and debris flow
505 cutting; (3) erosion, e.g., [sheet erosion, gully erosion and debris flow cutting](#); and (4) flow, e.g.,
506 [rock](#) avalanche and debris flow. The investigation on hotspots in the Wenchuan earthquake area,
507 Sichuan Province, suggests that the failure mode of the loose deposits was mostly of the slide
508 type, some of which may have occurred as rockfalls and erosion, and the fewest failures were
509 debris flows.

510 The [categories](#) of failure modes in landslide deposits proposed here can serve as a preliminary
511 hazard and risk assessment. More reliable assessments should consider the geotechnical
512 investigation method and means under various conditions and rely on accurate geological
513 analyses of landslide deposits. These massive deposits are still highly likely to induce geological
514 disasters under the effects of rainfall, earthquakes or human activities. Accordingly, the
515 prediction and stability evaluation of the deformation and damage of loose deposits formed by
516 strong earthquakes remain a matter of great concern.

517

518 *Acknowledgements*: This research was partially supported by the First batch of science and technology
519 planning projects of Jiangxi Provincial Department of Education Science and Technology Research
520 Project project (no.GJJ151124), Jiangxi province key research and development project
521 (no.20161BBG70051 & no.20171BBG70046), and National natural science foundation of China (no.
522 41641023 & no.51869012). We would like to express our gratitude to Prof. Huang Runqiu and Prof.
523 Pei XiangJun in Chengdu University of Technology, whose reviews helped improve this manuscript.

524

525 **References:**

526 Brian D. Collins, S.M.ASCE, and Dobroslav Znidarcic, M.ASCE.: Stability Analyses of Rainfall
527 Induced Landslides. *Journal of Geotechnical and Geoenvironmental Engineering*, 130, 362-372,
528 [https://doi.org/10.1061/\(ASCE\)1090-0241\(2004\)130:4\(362\)](https://doi.org/10.1061/(ASCE)1090-0241(2004)130:4(362)), 2004.

529 Tang, J. Zhu, W. L. Li, T. Liang.: Rainfall-triggered debris flows following the Wenchuan earthquake.
530 *Bull Eng Geol Environ*, 68, 187-174, DOI 10.1007/s10064-009-0201-6, 2009.

531 Cruden, D.M., Varnes, D.J.: Landslide types and processes, special report, transportation research
532 board, National Academy of Sciences, 247, 36-75, 1996.

533 Chai, H. J., Liu, H. C., & Zhang, Z. Y.: Landslide dams induced by Diexi earthquake in 1933 and its
534 environmental effect. *Journal of Geological Hazards and Environment Preservation*, 6, 7-17,1995.

535 Cui P., Zhu Y.Y., Han Y.S., Cheng X.Q., Zhang Jian-qi.: The 12 May Wenchuan earthquake-induced
536 landslide lakes distribution and preliminary risk evaluation. *Landslides*, 6, 209-223, DOI
537 10.1007/s10346-009-0160-9, 2009.

538 Cio P., Guo C.X., Zhou J.W., Hao M.H., Xu F.G.: The mechanisms behind shallow failure in slopes
539 comprised of landslide deposits. *Engineering Geology*, 180, 34-44,
540 <https://doi.org/10.1016/j.enggeo.2014.04.009>, 2014.

541 Fan X.M., Xu Q., Cee J. van Western, Huang R.Q., Tang R.: Characteristic and classification of
542 landslide dams associated with the 2008 Wenchuan earthquake. *Geoenvironmental Disasters*,12,79-87.
543 DOI 10.1186/s40677-017-0079-8, 2017.

544 Fan X.M., Xu Q., G. Scaringi, Dai L.X.: Li W.L., Dong X.J. Zhu X., et al.: Failure mechanism and
545 kinematics of the deadly June 24th 2017 Xinmo Landslide, Maoxian, Sichuan, China. *Landslides*, 14 ,
546 2129-2146, DOI 10.1007/s10346-017-0907-7, 2017.

547 Gan J.J., Huang R.Q, Li Q.Y., Ye X.H.and Gao WJ.: Characteristics and formation mechanism of
548 geo-hazards triggered by Wenchuan Ms8.0 Earthquake along Dujianyan to Wenchuan highway.
549 *Journal of Engineering Geology*, 18, 396-405, 2010.

550 Gan J.J., Sun H.Y., Huang R.Q., et al.: Study on mechanism of Formation and river blocking of
551 Hongchungou Giant Debris Flow at Yingxiu of Wenchuan County. *Journal of Catastrophology*, 27,
552 5-9, 2012.

553 Guo S.F., Qi S.W., Yang G.X., Zhang S.Z., Saroglou C.: An Analytical Solution for Block Toppling
554 Failure of Rock Slopes during an Earthquake, *Applied Sciences*, 10, 1-17, DOI 10.3390/app7101008,
555 2017.

556 Hu X.W., Huang R.Q., Zhu H.Y., Lu X.P., Zhang X., Shi Y.B.: Earthquake reactivation effects and
557 study of Malingyan landslide in Tanjiashan dammed lake. *Chinese Journal of Rock Mechanics and*
558 *Engineering*, 28, 1270-1279, 2009.

559 Huang R., and X. Fan.: The landslide story. *Nature Geoscience*, 5, 325-326, DOI: 10.1038/ngeo1806,
560 2013.

561 Huang R.Q.: Geohazard assessment of the Wenchuan earthquake. Beijing: Science Press, 2009.

562 Huang R.Q., Li W.L.: Fault effect analysis of geo-hazard triggered by Wenchuan earthquake. *Journal*
563 *of Engineering Geology*, 17, 19-28, DOI: 10.1007/s10064-009-0207-0, 2009.

564 Huang R.Q., Xu Q., Huo J.J.: Mechanism and geo-mechanics models of landslides triggered by 5.12
565 Wenchuan Earthquake. *Journal of Mountain Science*, 8, 2104-2113, DOI:
566 10.1007/s11629-011-2104-9, 2011.

567 Huang R.Q.: Large-scale landslides in China: Case studies. *Landslides and Engineered Slopes*-Chen et
568 al. (eds), 2037-2052, 2008.

569 Huang R.Q.: Understanding the Mechanism of Large-Scale Landslides, 2, 13-22, DOI:
570 10.1007/978-3-319-09057-3-2, 2015.

571 Hungr O, Evans S. G, Bovis M.J., et al.: A Review of the classification of landslides of the flow type.
572 *Environment and Engineering Geoscience*, VII(3) ,221-238, DOI: 10.2113/gseegeosci.7.3.221, 2001.

573 Hutchinson, J. N.: General Report: Morphological and geotechnical parameters of landslides in
574 relation to geology and hydrogeology. *Proceedings, Fifth International Symposium on Landslides* (Ed:
575 Bonnard, C.), 1, 3-35. Rotterdam: Balkema, 1988.

576 Hu W., Gianvito Scaring., Qiang Xu, and Runqiu Huan.: Internal Erosion Controls Failure and Runout
577 of Loose Granular Deposits: Evidence From Flume Tests and Implications for Postseismic Slope
578 Healing. *Geophysical Research Letters*, 5518-5527, <https://doi.org/10.1029/2018GL078030>, 2018.

579 Jack Morelock.: Shear Strength and Stability of Continental Slope Deposits Western Gulf of Mexico.
580 *Journal of Geophysical Research*, 74, 465-483, <https://doi.org/10.1029/JB074i002p00465>, 1969.

581 J. Dvorak and L. Novak.: Soil conservation and silviculture. Amsterdam; New York : Elsevier,
582 399, 1994.

583 Liao Z.H., Hong Y, Wang J, et al.: Prototyping an experimental early warning system for
584 rainfall-induced landslides in Indonesia using satellite remote sensing and geospatial datasets.
585 *Landslides* 7: 317–324. DOI: 10.1007/s10346-010-0219-7, 2010.

586 Kirschbaum D.B., Robert Adler, Yang Hong, Stephanie Hill, Arthur Lerner-Lam, Kramer S.L.: A
587 global landslide catalog for hazard applications: method, results, and limitations. *Nat Hazards*,
588 52:561–575, DOI 10.1007/s11069-009-9401-4, DOI 10.1007/s11069-009-9401-4, 2010.

589 Simth M.W.: Modified Newmark Model for Seismic Displacements of Compliant Slopes. *Journal of*
590 *Geotechnical and Geoenvironmental Engineering* 123(7), DOI: 10.1061/(ASCE)1090-0241, 123,
591 7(635), 635-644.1997.

592 Keefer, D.K.: Landslides caused by earthquakes. *Bulletin of the Geological Society of America*. 95,
593 406–421, 1984.

594 Matteo Albano, Michele S. Marco M., et al.: Minor shallow gravitational component on the Mt.
595 Vettore surface ruptures related to Mw 6, 2016 Amatrice earthquake. *Annals of Geophysics*. 59, 1-6,
596 DOI: <https://doi.org/10.4401/ag-7299>, 2016.

597 Meng W. L., Xu Y., Cheng W.C., Arulrajah A.: Landslide event on 24 June in Sichuan province,
598 China: Preliminary investigation and analysis. *Geosciences*, 8, 1-11, DOI:
599 10.3390/geosciences8020039, 2018.

600 Bauer, P. Neumann.: A guide to processing rock-fall hazard from field data.: Bundesanstalt für
601 Wasserbau.The 3rd International Symposium on Geotechnical Risk and Safety (ISGSR), 1-4, 2011.

602 Xu Q., Zhang S., Li W.L., Asch T.W.J.: The 13 August 2010 catastrophic debris flows after the 2008
603 Wenchuan earthquake, China. *Natural Hazards and Earth System Sciences*. 12, 201-216,
604 doi:10.5194/nhess-12-201-2012, 2012.

605 Xu Q., LI W.L., Dong X.J., Xiao X.X.: Fan X.M. Pei X.J.: The Xinmocun landslide on June 24, 2017
606 in Maoxian, Sichuan: characteristics and failure mechanism. *Chinese Journal of Rock Mechanics and*
607 *Engineering*. 11, 2612-2629, 2017.

608 Rens V. B., Erik L.H. C., Vicente A., Slobodan B. M.: Hillslope Processes: Mass Wasting, Slope
609 Stability and Erosion. *Slope Stability and Erosion Control: Ecotechnological Solutions*. DOI:
610 10.1007/978-1-4020-6676-4_3, 2008.

611 Ren J.J., Xu, X.W., Zhang, S.M., Liu S.: Surface rupture of the 1933 M7.5 Diexi earthquake in eastern
612 Tibet: Implication for seismogenic tectonics. *Geophysical Journal International*, 1:1627-1644, 2017.

613 R. Genevois et al.: Failure Mechanisms and Runout Behaviour of Three Rock Avalanches in North
614 Eastern Italian Alps. *Environmental Science & Engineering*, 9, 662-668, DOI:
615 10.1007/978-1-4020-4037-5_22, 2006.

616 Seed, H. B., & Martin, G. R.: The Seismic Coefficient of Earth Dam Design,” *Journal of the Soil*
617 *Mechanics and Foundations Division*, ASCE, Vol. 92, No. SM3, Proceedings Paper 4824, 25-48,
618 1966.

619 Sharpe. C. F. S.: *Landslides and Related Phenomena: A Study of Mass-Movements of Soil and Rock*:
620 Columbia University Press. New York. 137, 1938.

621 Sun Y.J., Zhang D., Shi B., Tong H. J., Wei G.Q., Wang X.: Distributed acquisition, characterization
622 and process analysis of multi-field information in slopes. *Engineering Geology*, 2, 49-62,
623 <https://doi.org/10.1016/j.enggeo.2014.08.025>, 2014.

624 Tang M.G., Xu Q, Huang R.Q.: Types of typical bank slope collapses on the three Gorges reservoir.
625 Journal of Engineering Geology, 2, 172-178, 2006.

626 Terzaghi, K.: Varieties of Submarine Slope Failure, NGI Publication No. 25: Norwegian Geotechnical
627 Institute,Oslo, 1956.

628 Tomáš P., Jan H., Jozef M., Oldrich H., Radek D.: Late Holocene catastrophic slope collapse affected
629 by deep-seated gravitational deformation in flysch: Ropice Mountain, Czech Republic.
630 Geomorphology, 3, 414-429, DOI: 10.1016/j.geomorph.2008.07.012, 2009.

631 Tarbuck, E.J., Lutgens, F.K.: Earth, an introduction to Physical Geology (6th ed.), Prentice Hall,
632 219-220, 1998.

633 Varnes D.J.: Slope movement types and processes. In: Schuster R.L. & Krizek R.J.Ed., Landslides,
634 analysis and control. Transportation Research Board Sp.Rep.No.176.Nat. Acad. Of Sciences, 11-33,
635 1978.

636 Varnes DJ (1954) Landslide types and processes. In: Eckel EB (ed) Landslides and engineering
637 practice, special report 28. Highway research board. National Academy of Sciences, Washington, DC,
638 pp. 20–47.

639 Wang S.J., Zhang J.M.: On the dynamic stability of block sliding on rock slopes. International
640 Conferences on Recent Advances in Geotechnical Earthquake Engineering and Soil Dynamics, 8,
641 431-434, 1981.

642 Yang, Z.H., Lan H.X., Liu H.J., Li L.P., Wu Y.M., Meng Y.S., Xu L.: Post-earthquake
643 rainfall-triggered slope stability analysis in the Lushan area. Journal of Mountain Science, 1, 232-242,
644 <https://doi.org/10.1007/s11629-013-2839-6>, 2015.

645 Yang Y.X., Li F.J., Chen T.H.: Analysis the Stability and Control Measures of the Suoqiao Sliding
646 Mass in Wenchuan, Sichuan Province. Geological Survey and Research, 3, 210-214, 2012.

647 Zhang S., Zhang L.M., Peng M., Zhang L.L., Zhao H.F., Chen H.X.: Assessment of risks of loose
648 landslide deposits formed by the 2008 Wenchuan earthquake. Natural Hazards and Earth System
649 Sciences, 12, 1381-1392, doi:10.5194/nhess-12-1381-2012, 2012.